Report on Late Paleozoic bimodal volcanic associations discovered in Northern Mongolian Rift zone

Yuri D Shcherbakov, Alexander B Perepelov, Svetlana S Tsypukova

Citation: Yuri D Shcherbakov, Alexander B Perepelov, Svetlana S Tsypukova, 2020. Report on Late Paleozoic bimodal volcanic associations discovered in Northern Mongolian Rift zone, China Geology, 3, 496–500. doi: 10.31035/cg2020033.

View online: https://doi.org/10.31035/cg2020033

Related articles that may interest you

Genesis of pyroxenite veins in supra–subduction zone peridotites: Evidence from petrography and mineral composition of Egiingol massif (Northern Mongolia)

China Geology. 2020, 3(2), 299 https://doi.org/10.31035/cg2020035

Prospective prediction and exploration situation of marine Mesozoic–Paleozoic oil and gas in the South Yellow Sea

China Geology. 2019, 2(1), 67 https://doi.org/10.31035/cg2018072

A new alvarezsaurid dinosaur from the Late Cretaceous Qiupa Formation of Luanchuan, Henan Province, central China

China Geology. 2018, 1(1), 28 https://doi.org/10.31035/cg2018005

Mafic–ultramafic magma activity and copper–nickel sulfide metallogeny during Paleozoic in the Eastern Kunlun Orogenic Belt, Qinghai Province, China

China Geology. 2019, 2(4), 467 https://doi.org/10.31035/cg2018124

Characteristics of tectonic deformation of the melange zone in the Lachlan Orogen along eastern coast of Australia

China Geology. 2019, 2(4), 478 https://doi.org/10.31035/cg2018131

Sediment distribution and provenance since Late Pleistocene in Laizhou Bay, Bohai Sea, China

China Geology. 2019, 2(1), 16 https://doi.org/10.31035/cg2018062

China Geology 3 (2020) 496−500

China Geology

Journal homepage: http://chinageology.cgs.cn
https://www.sciencedirect.com/journal/china-geology

Research Advances

Report on Late Paleozoic bimodal volcanic associations discovered in Northern Mongolian Rift zone

Yuri D Shcherbakov*, Alexander B Perepelov, Svetlana S Tsypukova

Vinogradov Institute of Geochemistry Siberian Branch of Russian Academy of Science, Irkutsk 664033, *Russia*

1. Objectives

Within the Northern-Mongolian –Transbaikalian Rift system, bimodal volcanic associations with felsic agpaitic rocks are widespread, often accompanied by alkaline granites plutons. There are two segments in the Rift system structure –Northern-Mongolian with length of 600 km and Western-Transbaikalian with length of 800 km on latitude. Most western appearances of alkaline granites and bimodal magmatism are Bat-Tsengel, Upper-Hanui and Orkhont plutons (Vorontsov AA et al., 2007). Volcanic rocks typical for the bimodal series of these locations are basaltic trachyandesites, trachyandesites, phonolites, trachytes and trachyrhiolites presented in various combinations. At the same time, the least studied area of this structure within the North Mongolian segment to date was its Northern flank. During the expeditions of 2016 –2019 years, discovered dike swarm predominantly consists of pantellerites, rare pantelleritic trachytes and trachybasalts. Such factors as absence of data on bimodal magmatism appearance in this region, mainly pantelleritic composition of dike swarm rocks make a research results relevant for solving the North Mongolian segment of the Rift zone bimodal series origin. Late Paleozoic age of the dike belt estimated according to Northern flank of the Rift zone geochronolgical data by Vorontsov AA et al. 2007.

The studied dike belt stretch across the Delger-Muren River close to Tsagaanuul village in the Hujirtgol, Buyantgol, Shargagol rivers basin. Dikes has general Northeast strike and confined to a large fault structure. Dike swarm named Tsgaanuul as closest village (Fig. 1). Dikes break through large Middle Paleozoic granite pluton and on the Northeast through Cambrian meta-sandstone strata. The Southwest part of the dike swarm overlaid by Neogene basalts. Contact with host rocks is intrusive, with the presence of granite xenoliths in dike contact zones. Dike relicts are 5–6 m tall, sub-volcanic bodies width varies from 1 m to 8 m (Fig. 2), length of some dikes reaches 7 km. There is zonality in large pantelleritic dikes, from central to apical zones rocks structure changes from medium grained to fine grained and glassy. For some dikes in their apical zones, observe the release of large sanidine crystals up to 5–7 mm in size. Dikes of pantelleritic trachytes are rare, largest dike has thickness of 4 m and a general Northeastern strike coinciding with the strike of pantellerite dikes and a large fault (Fig. 2). The pantelleritic trachytes structure varies from mid grained to fine grained. There is rare observation of “dike in dike” structure it is when pantelleritic trachytes within one sub-volcanic body broke by pantellerite dike. Trachybasalts dykes of the studied bimodal series appear in the southeastern flank of the swarm and have northeastern strike different from pantellerites on 15º –20º. Thickness of the trachybasalts dikes is up to 2 m, and sometimes spacing between dikes is around 4 m. Trachybasalts characterize by significant secondary changes, and rare sulphide mineralization. With intrusive contact pantelleritic trachytes and pantellerites breaks through trachybasalts dikes.

2. Methods

Sixty samples of pantellerites, trachytes and trachybasalts were studied. Analytical studies were conducted in the center of collective use “Isotope-geochemical research ” IGC SB RAS. Major oxides contents determine with XRF method on multichannel X-Ray spectrometer SRM-25 (“Orelnauchpribor” Russia). Measurements made using an X-Ray tube with Rh anode at a voltage of 30 kV and a current of 40 mA. The

* Corresponding author: *E-mail address*: scherb@igc.irk.ru (Yuri D. Shcherbakov).

doi:10.31035/cg2020033
2096-5192/© 2020 China Geology Editorial Office.

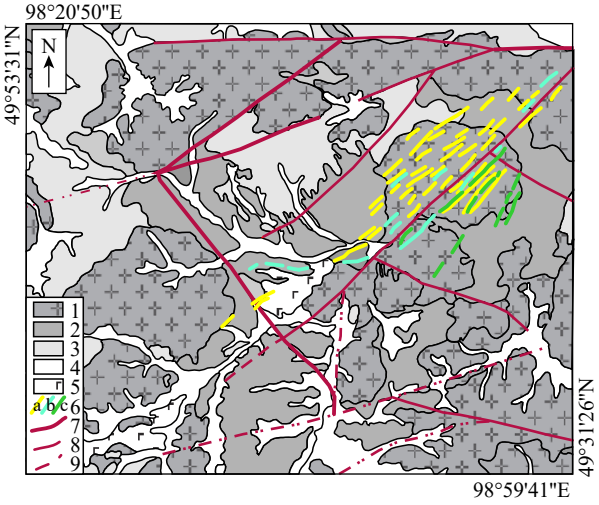

Fig. 1. Geological scheme of Tsagaanuul dike swarm. 1–Pz_2 intrusive complex (granites and granitoids); 2–V-Є deposits (sandstones siltstone, pelit, gravelite); 3–Cambrian system (meta sandstones, limestones, quartzites); 4–Upper Quaternary (modern sediments. Deluvially proluvial rubble); 5–Neogene basalts; 6–dikes of pantellerites (a), pantelleritic trachytes (b), trachybasalts (c); 7–breaking faults; 8–alleged breaking faults; 9–alleged breaking faults under quaternary sediments.

samples homogenized by fusion with flux, lithium metaborate ($LiBO_2$) in an induction furnace in glass-carbon crucibles at a temperature of 1100ºC. Quality control of major oxides definitions was carried out using standard samples SG-1A (granite, Russia), SG-2 (granite, Russia) and JG-2 (granite, Japan). Trace element concentrations in the samples obtained by inductively coupled plasma ionization mass spectrometry (ICP-MS). Measurements carried out on mass spectrometers with magnetic sector ELEMENT 2 (Finnigan MAT, Germany) with double focus and signal registration in three resolutions: Low (LR)-300, medium (MR)-4000 and high (HR)-10000 M/ΔM and quadrupole spectrometer NexION 300D by Perkin Elmer (USA). The correct determination of trace element concentrations and instrument drift monitored by international standard samples of basalts BHVO-1, BHVO-2 (USGS) and andesites AGV-1, AGV-2 (USGS) every 5–6 samples.

Additional rocks trace element composition determinations carried out on the quadrupole mass spectrometer Agilent 7700 x firm Agilent Technologies ("Baikal center of Nanotechnology", Technopark at Irkutsk

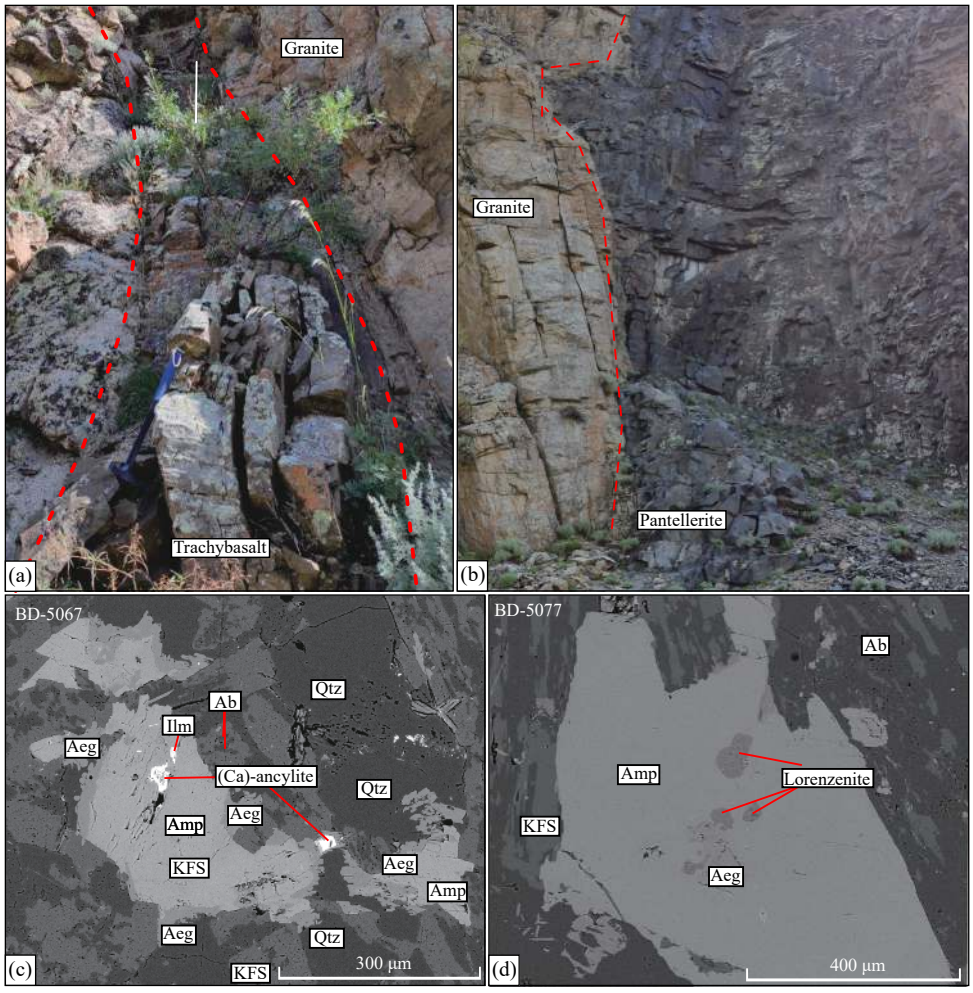

Fig. 2. Dikes of trachybasalts (a) and pantellerites (b) field photos and backscattered electrons (BSE) images (c and d) of common mineral assemblages in pantellerites (BD-5067) and trachytes (BD-5077). Ab–albite, Aeg–aegirine, Amp–amphibole, Ilm–ilmenite, KFS–potassic feldspar, Qtz–quartz.

national research technical University).

The study of rock-forming mineral compositions carried out on the electron microscope "LEO 1430VP" (Carl Zeiss, Germany) with the analyzer "Inca Energy 300 " (Oxford Instruments Ltd. Czech Republic) (Geological Institute SB RAS Ulan-Ude) and MIRA 3LMU (Tescan Ltd. Holland) with the energy-dispersion spectrometer INCA Energy-450+ (Oxford Instruments Ltd, England) (Sobolev 's Institute of Geology and Mineralogy SB RAS.) at an accelerating voltage of 15–20 kV and a current of about 0.5 nA (probe size <1 μm, spectrum set time 10–50 sec).

3. Results

Major phenocysts for the dike swarm pantellerites and pantelleritic trachytes are feldspars, amphiboles and quartz. Amphiboles are from Na-Ca subgroup and define as arfvedsonite, kataphorite and richteritte. There are rare crystals of Ca amphibole – edenite. Amphiboles of the dike swarm felsic rocks feature are enrichment in Ti and Fe. Pantelleritic trachytes clinopyroxenes represented aegirine and augite, however in pantellerites clinopyroxenes represented only by aegirine. Both rock types characterized by pyroxene occurrence as intergrowth with amphibole or as microlite in a groundmass, often with mixture of ZrO_2 (up to 6%). Pantelleritic trachytes characterize by presence of aenigmatite in the intergrowth of kataphorite and aegirine, also by occurrence of rare for agpaitic rocks mineral–lorenzenite ($Na_2Ti_2Si_2O_9$) as inclusion in amphibole. In the dike swarm rocks Zr-bearing minerals such as elpidite (ZrO_2 up to 31%), ctatpleiite (ZrO_2 up to 19%), product of eudialite group minerals alteration (ZrO_2 up to 26%) are widespread. Feldspars represented by albite and sanidine splices with limiting compositions (Ab_{100}-Or_{100}). In rocks, REE minerals are widespread among microliths appearance of monazite and apatite, Ca-ancyllite in pantellerites is noted. Phenocrysts of trachybasalts represented by clinopyroxene and plagioclase.

Major oxides concentrations distribution shows bimodal character of dike swarm series (Fig. 3). Felsic alkaline rocks compositions on graph FeO* versus Al_2O_3 shows accordance of composition to pantellerites and pantelleritic trachytes (Fig. 3a). Group of points between pantellerites and trachytes is pantellerites with sanidine megacrysts. The maximum of agpaitic index (molar (Na+K)/Al)) for pantelleritic trachytes is 1.2 and for pantellerites is 1.4, what combined with presence of alkaline amphiboles, aegirine along with aenigmatite, catapleiite, elpidite, lorenzenite allow to classify

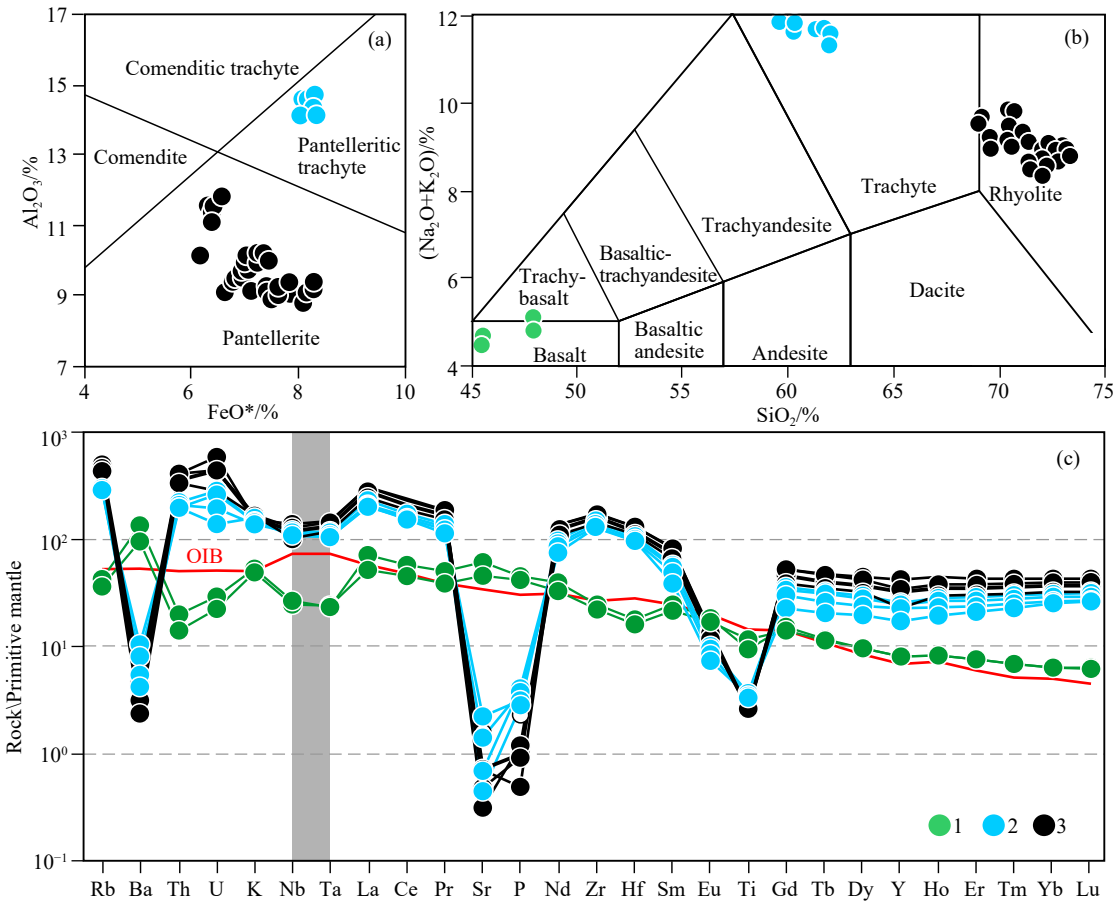

Fig. 3. Diagrams of FeO *vs.* Al_2O_3 (a); SiO_2 *vs* Na_2O+K_2O (b) and spider diagrams (c) for the dike swarm rocks. *Notes:* 1–trachybasalts; 2–pantelleritic trachytes; 3–pantellerites. Trace elements concentrations normalized to primitive mantle (after Sun SS and McDonough, 1989). OIB composition (after Thompson RN et al., 1984).

the dike swarm rocks as alkaline and agpaitic (Marks MAW and Gregor MA. 2017). Trachybasalts belong to normal alkalinity range. Compare to trachybasalts in pantelleritic trachytes and pantellerites there are depletion of TiO_2, Al_2O_3, FeO, MgO, CaO, and P_2O_5 concentrations occurs alkalinity reaches its maximum in pantelleritic trachytes (Table 1). On the ratio of Na_2O/K_2O, pantellerites have approximately equal ratio of Na_2O and K_2O (Na_2O/K_2O=0.9 –1.1), whereas in trachybasalts (Na_2O/K_2O=1.6–2.3) and pantelleritic trachytes (Na_2O/K_2O=1.2–1.6) predominantly sodic alkalinity character (Fig. 3b).

Trace elements distributions on spider-diagrams show that for all rocks of bimodal series characterized by presence of small Nb-Ta minimum. Trachybasalts depleted with HFSE, Th and U, and this signs differ them from OIB along with enrichment with Ba, Sr and P (Fig. 3c). Pantelleritic trachytes and pantellerites are close to each other on trace elements distribution pattern, and have depletion with Ba, Sr, P, Eu.

4. Conclusion

Established geochemical features of Tsagaanuul dike swarm bimodal association suggest that alongside deep source a metasomatized mantle matter altered during previous subduction events take a part, this indicated by HFSE depletion. Genetic connections with pantelleritic trachytes and pantellerites from one side and trachybasalts from the other

Table 1. Major elements (%) and trace element compositions (10^{-6}) compositions of representative Tsagaanul dike swarm rocks.

No.	EM1902 1	EM1907	EM1903 2	EM1001	BD5077	EM1911 3	EM1003	EM1011	BD5075	BD5066	BD5062
SiO_2	45.30	45.37	60.17	61.92	61.56	72.56	71.94	72.09	72.18	72.49	72.85
TiO_2	2.34	1.89	0.74	0.77	0.71	0.48	0.52	0.53	0.53	0.51	0.53
Al_2O_3	15.37	14.81	14.32	14.68	14.66	9.06	9.50	9.96	9.10	9.08	9.63
Fe_2O_3	12.21	10.90	9.30	9.32	9.32	7.44	7.67	7.85	7.99	8.32	7.75
MnO	0.21	0.17	0.28	0.29	0.28	0.16	0.15	0.16	0.19	0.21	0.19
MgO	4.96	5.39	0.97	0.32	0.36	0.01	0.05	0.06	0.05	0.05	0.06
CaO	8.10	8.24	1.23	1.47	1.13	0.31	0.50	0.43	0.44	0.46	0.39
Na_2O	3.21	2.94	7.22	6.25	6.79	4.30	4.03	4.31	4.51	4.44	4.18
K_2O	1.39	1.51	4.93	5.04	4.94	4.43	4.53	4.58	4.43	4.43	4.55
P_2O_5	0.84	0.92	0.10	0.07	0.06	0.02	0.03	0.02	0.02	0.02	0.04
LOI	4.57	7.02	0.63	0.46	0.48	0.47	0.38	0.36	0.60	0.40	0.31
Total	98.68	99.35	100.03	100.58	100.29	99.48	99.30	100.36	100.05	100.40	100.48
Rb	20.9	24.7	202	194	199	303	260	262	292	286	280
Sr	896	1193	21.2	45.9	9.05	9.05	16.4	6.18	9.57	13.5	7.11
Y	34.3	34.8	123	113	117	129	126	98.5	147	139	129
Zr	232	256	1764	1509	1525	1311	1529	1490	1801	1596	1772
Nb	16.0	17.5	83.1	82.1	84.6	77.0	71.9	68.5	85.2	70.0	79.0
Cs	4.24	2.24	3.10	3.63	4.25	1.29	1.98	1.86	2.99	1.80	1.18
Ba	625	867	17.4	73.4	28.8	15.5	20.5	15.7	21.6	24.7	27.2
La	33.5	46.0	158	148	162	181	165	160	202	153	189
Ce	75.4	96.5	322	302	320	383	329	320	402	305	370
Pr	9.79	12.6	38.0	35.4	38.1	41.5	39.5	39.5	48.6	36.9	45.3
Nd	41.0	49.5	133	121	132	145	138	138	171	132	160
Sm	8.59	9.99	25.6	23.9	25.0	27.1	27.2	26.5	33.7	25.8	31.0
Eu	2.57	2.76	1.72	1.56	1.68	2.12	1.91	1.80	2.16	1.58	2.19
Gd	7.59	8.12	21.2	19.5	21.0	22.1	22.5	21.0	28.7	22.7	25.6
Tb	1.11	1.14	3.47	3.29	3.43	3.58	3.66	3.50	4.62	3.76	4.22
Dy	6.42	6.44	21.0	20.4	21.6	21.9	22.9	21.8	28.2	23.8	25.8
Ho	1.22	1.22	4.39	4.26	4.51	4.59	4.69	4.43	5.72	5.04	5.34
Er	3.31	3.30	12.9	12.5	13.6	13.8	13.7	13.3	16.7	15.1	15.5
Tm	0.46	0.46	1.97	2.01	2.16	2.20	2.14	2.11	2.65	2.31	2.43
Yb	2.80	2.77	13.5	13.5	14.4	14.8	14.4	14.3	17.6	15.5	16.4
Lu	0.42	0.42	2.14	2.09	2.22	2.23	2.25	2.19	2.71	2.46	2.48
Hf	4.48	5.05	31.9	30.5	32.6	25.1	30.6	31.5	37.5	33.7	36.8
Ta	0.88	0.86	4.30	4.30	4.60	4.52	4.31	4.37	5.38	4.34	5.07
Pb	7.02	8.35	47.5	46.6	49.8	36.9	47.5	51.3	63.0	58.5	61.0
Th	1.11	1.55	19.1	18.0	19.2	32.2	26.9	26.7	32.3	24.2	25.5
U	0.44	0.57	5.33	4.25	6.24	9.08	7.66	5.69	8.88	8.87	7.14

Notes: 1–trachybasalts, 2–trachytes, 3–pantellerites. All iron presented as Fe_2O_3.

side can be consider within the framework of the hypothesis of deep magma source evolution (Kozlovsky AM et al., 2007). Long-term differentiation of magmas in the source is possible with participation of their crystallization and melt separation processes allow explaining the bimodal nature distribution of their compositions.

CRediT authorship contribution statement

Shcherbakov Yuri D and Perepelov AB conceived of the presented idea. Shcherbakov Yuri D performed the computations, verified the analytical methods and prepared manuscript. Perepelov AB supervised the findings of this work. Tsypukova SS contributed to manuscript verification. All authors collected and preparing samples for analysis discussed the results and contributed to the final manuscript.

Declaration of competing interest

The authors declare no conflicts of interest.

Acknowledgment

The reported study was funded by RFBR according to the research projects (18-35-00294, 18-55-91049).

References

Kozlovsky AM, Yarmolyuk VV, Kovalenko VI, Savatenkov VM, Velivetskaya TA. 2007. Trachytes, comendites, and pantellerites of the Late Paleozoic bimodal rift association of the Noen and Tost Ranges, Southern Mongolia: Differentiation and contamination of peralkaline salic melts. Petrology, 15(3), 240–263. doi: 10.1134/S0869591107030034.

Marks MAW, Gregor MA. 2017. Global review on agpaitic rocks. Earth-Science Reviews, 173, 229–259. doi: 10.1016/j.earscirev.2017.06.002.

Sun SS, McDonough WF. 1989. Chemical and isotopic systematics of oceanic basalts: Implications for mantle composition and processes. Geological Society London Special Publications, 42(1), 313–345. doi: 10.1144/GSL.SP.1989.042.01.19.

Thompson RN, Morrison MA, Hendry GL, Parry SJ. 1984. An assessment of the relative roles of crust and mantle in magma genesis: An elemental approach. Philosophical Transactions of the Royal Society A, 310(1514), . doi: 10.1098/rsta.1984.0008.

Vorontsov AA, Dril SI, Tatarnikov SA, Sandimirova GP, Yarmolyuk VV, Lykhin DA. 2007. Magmatic sources and geodynamics of the early Mesozoic Northern Mongolia-Western Transbaikalia rift zone. Petrology, 15(1), 35–57. doi: 10.1134/S0869591107010031.